

ADVANCED MATERIALS

Supporting Information

for *Adv. Mater.*, DOI: 10.1002/adma.201403907

High-Performance Magnetic Sensorics for Printable and Flexible Electronics

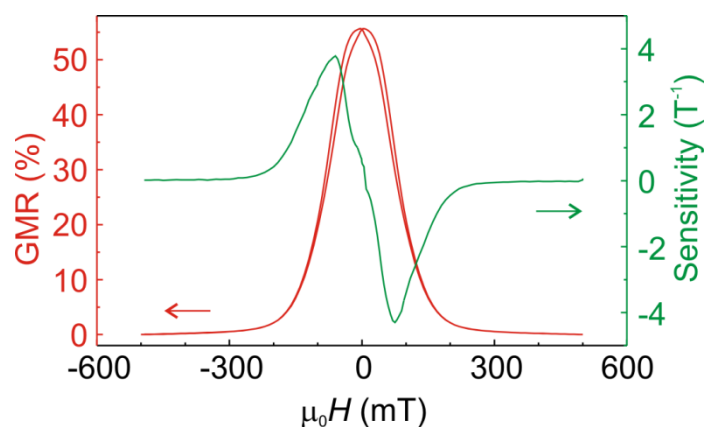
*Daniil Karnaushenko, * Denys Makarov, * Max Stöber, Dmitriy D. Karnaushenko, Stefan Baunack, and Oliver G. Schmidt*

Supporting Information

High performance magnetic sensorics for printable and flexible electronics

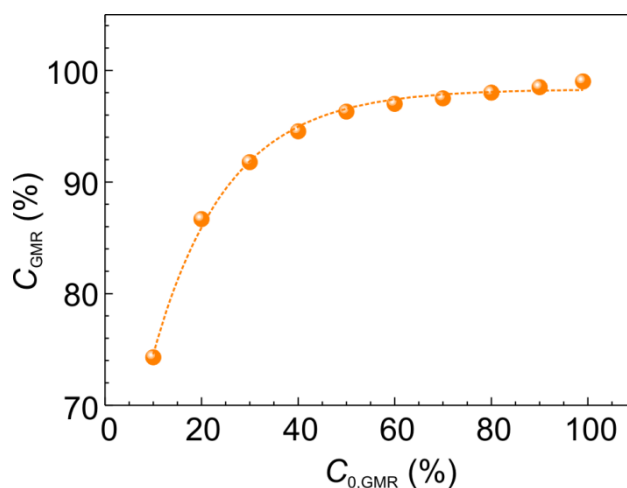
Daniil Karnaushenko*, Denys Makarov*, Max Stöber, Dmitriy Karnaushenko, Stefan Baunack, Oliver G. Schmidt

(A) Magneto-electric characterization of the as-deposited Co/Cu GMR multilayer stack.



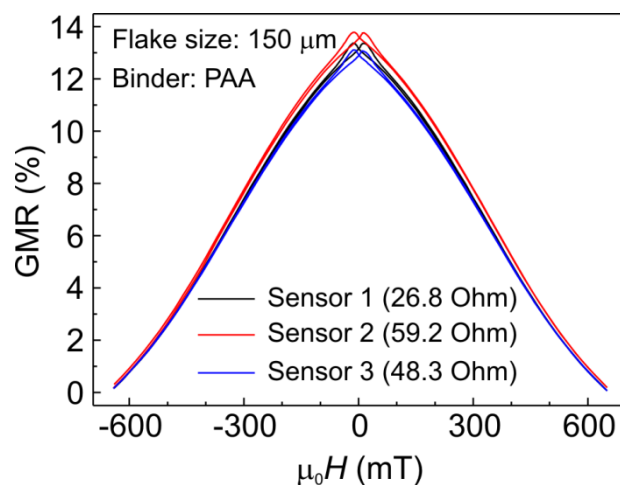
Supporting Figure S1. GMR curve of the Co/Cu multilayer stacks prepared on rigid SiOx wafer by sputter deposition. The field dependent sensitivity of the GMR sensors is also shown.

(B) Content of the GMR powder in the dried binder.



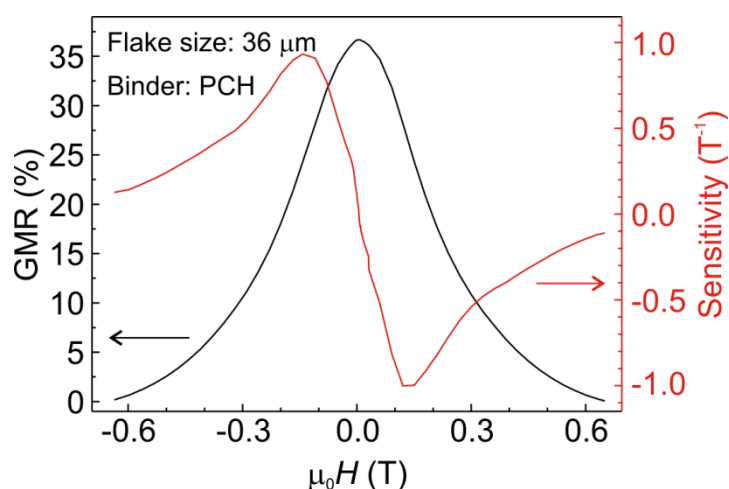
Supporting Figure S2. Concentration of the GMR powder in the dried binder, C_{GMR} , with respect to the initial concentration of the GMR powder added to the liquid binder solution, $C_{0,GMR}$.

(C) Reproducibility of the magneto-electrical performance of the sensors prepared in a single run.



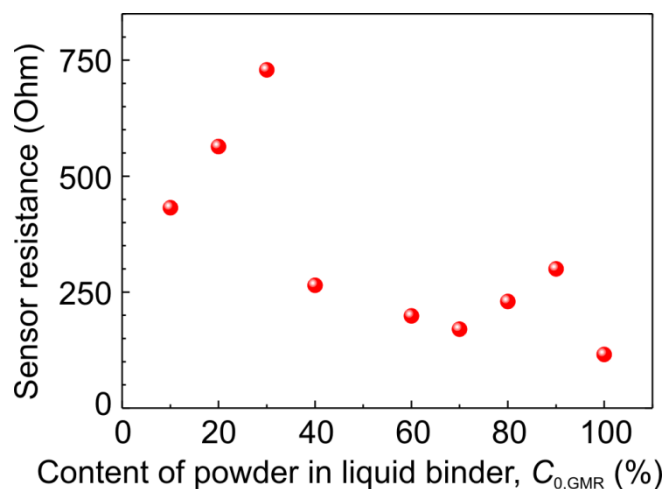
Supporting Figure S3. Comparison of the GMR performance taken of 3 sensors prepared by a brush painting method on FPC. PAA based binder solution was used in this study. The concentration of GMR powder in the binder is 95%.

(D) Sensitivity of the GMR sensor printed onto a flexible printed circuit board.



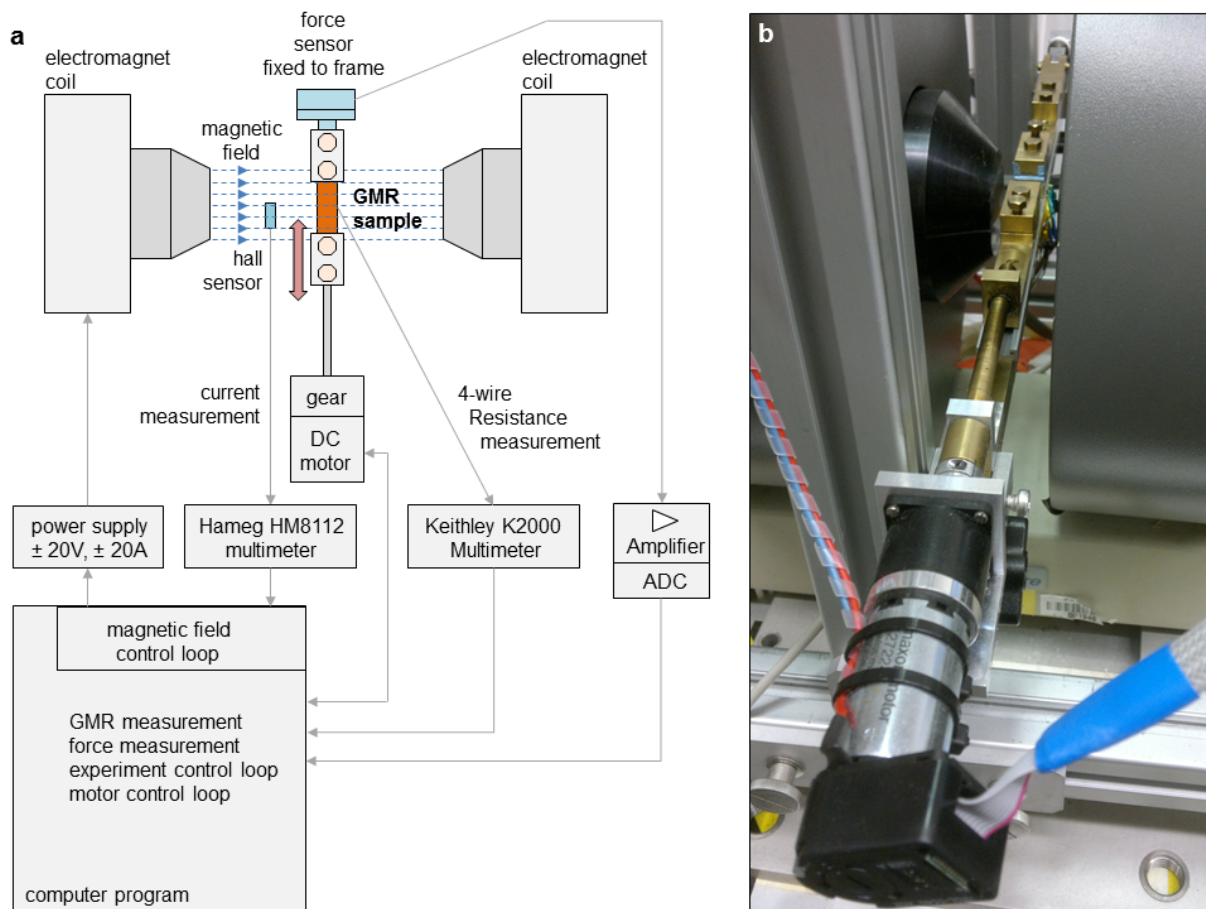
Supporting Figure S4. GMR curve of the Co/Cu multilayer stacks printed on FPC. The field dependent sensitivity of the GMR sensors is also shown (filled triangles). PCH based binder solution was used in this study. The size of the GMR flakes is 36 μm . The concentration of GMR powder in the binder is 99%.

(E) Change of the sensor resistance with the concentration of the GMR powder in the binder solution.



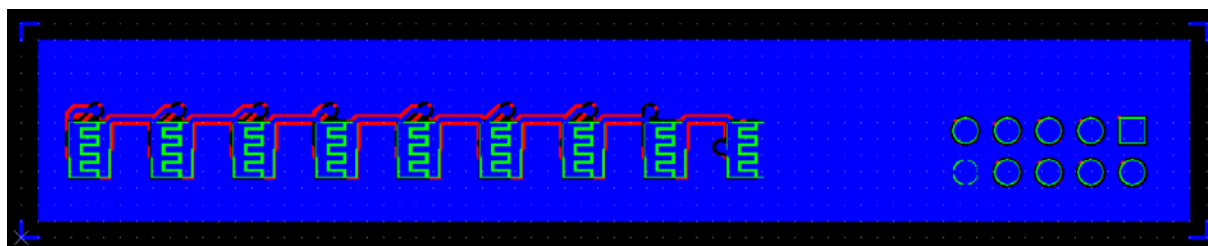
Supporting Figure S5. Change of the sensor resistance upon the concentration of the GMR powder in the liquid binder solution, $C_{0,GMR}$.

(F) Setup for the *in situ* bending tests.



Supporting Figure S6. The *in situ* bending setup. (a) Schematic view of the setup. (b) Photograph of the motorized stretching stage between the pole shoes of the electromagnet.

(G) Layout of the flexible printed circuit board (FPC).



Supporting Figure S7. The FPC accommodates 9 independent sensor locations each consisting of a finger pattern. The distance between the electrodes and the width of an electrode is 250 μm .